Multiplexed Enrichment and Detection of Malarial Biomarkers Using a Stimuli-Responsive Iron Oxide and Gold Nanoparticle Reagent System

Michael A. Nash,[†,§] John N. Waitumbi,[‡] Allan S. Hoffman,[†] Paul Yager,[†] and Patrick S. Stayton[†,*]

[†]Department of Bioengineering, University of Washington, Seattle, Washington 98195, United States and [‡]Walter Reed Project, Kenya Medical Research Institute, Kisumu, Kenya. [§]Present address: Lehrstuhl für Angewandte Physik and Center for NanoScience, Ludwig-Maximilians-Universität, D-80799 Munich, Germany

ABSTRACT There is a need for simple yet robust biomarker and antigen purification and enrichment strategies that are compatible with current rapid diagnostic modalities. Here, a stimuli-responsive nanoparticle system is presented for multiplexed magneto-enrichment and non-instrumented lateral flow strip detection of model antigens from spiked pooled plasma. The integrated reagent system allows purification and enrichment of the gold-labeled biomarker half-sandwich that can be applied directly to lateral flow test strips. A linear diblock copolymer with a thermally responsive poly(*N*-isopropylacrylamide) (pNIPAm) segment and a gold-binding block composed of NIPAm-*co*-*N*,*N*-dimethylaminoethylacrylamide was prepared by reversible addition–fragmentation chain transfer polymerization. The diblock copolymer was used to functionalize gold nanoparticles (AuNPs), with subsequent bioconjugation to yield thermally responsive pNIPAm-AuNPs that were co-decorated with streptavidin. These AuNPs efficiently complexed biotinylated capture antibody reagents that were bound to picomolar quantities of pan-aldolase and *Plasmodium falciparum* histidine-rich protein 2 (PfHRP2) in spiked pooled plasma samples. The gold-labeled biomarker half-sandwich was then purified and enriched using 10 nm thermally responsive magnetic nanoparticles that were similarly decorated with pNIPAm. When a thermal stimulus was applied in conjunction with a magnetic field, coaggregation of the AuNP half-sandwiches with the pNIPAm-coated iron oxide nanoparticles created large aggregates that were efficiently magnetophoresed and separated from bulk serum. The purified biomarkers from a spiked pooled plasma sample could be concentrated 50-fold into a small volume and applied directly to a commercial multiplexed lateral flow strip to dramatically improve the signal-to-noise ratio and test sensitivity.

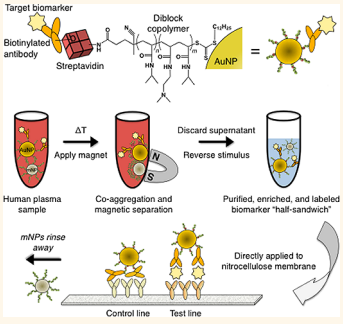

KEYWORDS: magnetic · gold · nanoparticles · diagnostics · immunochromatography · malaria

The lateral flow assay is a currently dominant point-of-care technology for distributed and low resource settings that rapidly detects biomarkers and antigens in bodily fluids (*e.g.*, blood, urine).[1−8] A primary limitation of this technology, however, is that the range of sensitivity and targets is restricted to antigens of relatively high abundance in the plasma.[9] There is thus a need for simple purification and enrichment strategies that can be employed in the same distributed settings to improve test sensitivity while leveraging the success and widespread acceptance of lateral flow rapid diagnostic tests.

Thermally responsive polymers (*e.g.*, poly(*N*-isopropylacrylamide), pNIPAm) have been widely investigated as separation/enrichment systems for affinity purification of biomolecules when conjugated to macromolecules such as proteins[10,11] or nucleic acids.[12,13] Magnetic particles represent a separate yet complementary separation/enrichment technology that has commonly been used for sample preparation in the clinical laboratory[14,15] and microfluidics fields.[16,17] Our group recently reported on stimuli-responsive small (10 nm) iron oxide magnetic nanoparticles (mNPs) with a pNIPAm corona that directed thermally triggered aggregation and rapid magnetophoresis of captured targets in a modest field.[18] The small size of the mNPs facilitated mass transport and rapid binding of targets to the particles, which proved useful for continuous flow purification and concentration of model diagnostic targets.[19]

More recently, we have demonstrated ways to incorporate the high-efficiency visible light extinction properties of gold nanoparticle reagents (AuNPs) into thermally responsive magnetic nanoparticle separation systems. The first of these systems was a core–shell system where we incorporated amine groups into a diblock copolymer design.[20] Iron oxide core nanoparticles stabilized by the diblock copolymers retained the amine groups on the surface, which under appropriate conditions reduced gold

* Address correspondence to stayton@u.washington.edu.

Received for review April 5, 2012 and accepted July 17, 2012.

Published online July 17, 2012
10.1021/nn3015008

ions in solution, forming a gold shell. This system, however, was found to have limitations associated with slow magnetophoresis.

The design of the second separation system[21] was based on the observation that coaggregation of thermally responsive nanoparticle mixtures can achieve high-efficiency magnetic separation of nonmagnetic nanoparticles. Thus, rapid magnetic separation of the gold-labeled biomarkers was achieved in a simple mixture of two different types of thermally responsive nanoparticles, where each particle type (gold or magnetic) could be optimized independently, and the stoichiometric ratios could be precisely controlled to tune the magnetophoresis behavior.

This mixed nanoparticle separation system is shown here to achieve magneto-enrichment of AuNP "half-sandwich" malaria antigen immunocomplexes. The AuNP-antigen half-sandwich is the active detection species used to visualize disease diagnosis in conventional lateral flow tests. The mixed nanoparticle system design allows the rapid and simple magnetic separation of target antigens but does not yield a magnetic nanoparticle-bound biomarker like conventional magnetic bead separations. The separated and concentrated biomarker-AuNP half-sandwich is directly produced and thus able to accommodate binding to the second capture antibody at the test line of the lateral flow strip or dipstick. Volumetric enrichment of malarial biomarkers is shown from larger pooled plasma volumes to achieve higher analytical sensitivity in a non-instrumented and multiplexed strip test format.

RESULTS AND DISCUSSION

Polymer Synthesis and Characterization. The diblock copolymer used to functionalize the gold nanoparticle detection reagent was synthesized by reversible addition−fragmentation chain transfer (RAFT) polymerization. The polymer design incorporated a thermally responsive pNIPAm block and a cationic p(NIPAm-*co*-DMAEAm) random copolymer block to drive polymer adsorption onto citrate-stabilized AuNPs. Size exclusion chromatography with multiangle light scattering detection showed that the homo-pNIPAm polymer had a molecular weight M_n = 17.1 kDa, with polydispersity index PDI = 1.04, and d*n*/d*c* of 0.076. Diblock chain extension with a short random copolymer block of NIPAm and DMAEAm (*N*,*N*-dimethylaminoethylacrylamide) was performed using the 17.1 kDa homo-pNIPAm polymer as a macro-chain-transfer agent in methanol. Size exclusion chromatography showed that the diblock copolymer had M_n = 21.5 kDa, PDI = 1.11, and d*n*/d*c* of 0.071. The chemical shifts of the DMAEAm protons were dependent on the protonation state of the tertiary amine groups in the polymer, consistent with the previous study.[20] The ^{1}H NMR spectrum of the diblock copolymer can be found in the online Supporting Information (Supplementary Figure 1). The ionizable DMAEAm amine groups in the second block caused the diblock copolymer to have a pH-dependent thermal aggregation profile (Supplementary Figure 2).

Gold Nanoparticle Synthesis and Surface Modification. Negatively charged gold nanoparticles were synthesized using trisodium citrate as a reducing agent and stabilizing ligand. Following AuNP synthesis, the reaction mixture was cooled and the pH raised to 8.2, near the pK_a of the DMAEAm monomer. The diblock copolymer in DI water was then added and adsorbed onto the gold colloid overnight. After 24 h, NaCl was added up to 125 mM to shield electrostatic interactions. No particle flocculation occurred, indicating successful particle stabilization. Incorporating a cationic polymer segment greatly facilitated AuNP colloidal stability in physiological buffers and prevented salt-induced particle flocculation better than trithiocarbonate or secondary thiol-terminated homo-pNIPAm polymers of equivalent molecular weight. Recently, however, it was reported that small molecule trithiocarbonates are capable of forming self-assembled monolayers on gold surfaces with densities similar to alkane thiols.[22] It may be possible that, in addition to electrostatic interactions, chemisorption of the sulfur-containing RAFT polymer end group also plays a role in successful surface modification of the AuNPs by the diblock copolymer.

Conjugation of AuNPs to Streptavidin (SA). After successful modification of the AuNPs with polymer, the end carboxyl group was conjugated to lysine amine groups on streptavidin using carbodiimide chemistry, forming the product SA-AuNPs. Membrane ultrafiltration was used to remove nonconjugated streptavidin from the reaction mixture. As shown in Supplementary Figure 3, after three rounds of ultrafiltration, no streptavidin absorbance at 280 nm was measured from the filtered particle eluent, indicating that all of the nonconjugated streptavidin had been removed. Confirmation of streptavidin conjugation to the gold particles was provided by flowing the SA-AuNPs through a nitrocellulose flow strip that had been modified with a stripe of anti-streptavidin IgG (Abcam, product #AB6676). As the SA-AuNPs flowed through the capture zone, the accumulation of red color at the location of IgG surface modification confirmed streptavidin modification of the AuNP-pNIPAm reagent.

Biotinylation of IgG Antibodies. A commercial NHS-chromogenic-biotin was conjugated to lysine amine groups on the IgG capture antibodies. After conjugation and purification, the ratio of chromophore linker absorbance at 354 nm to IgG absorbance at 280 nm was used to estimate the degree of biotinylation. For the anti-PfHRP2 IgG, a 1:20 dilution of the antibody showed A_{280}/A_{354} = 0.116/0.068. Given the chromogenic-biotin extinction coefficient of ε = 29 000 M^{-1} cm^{-1} at

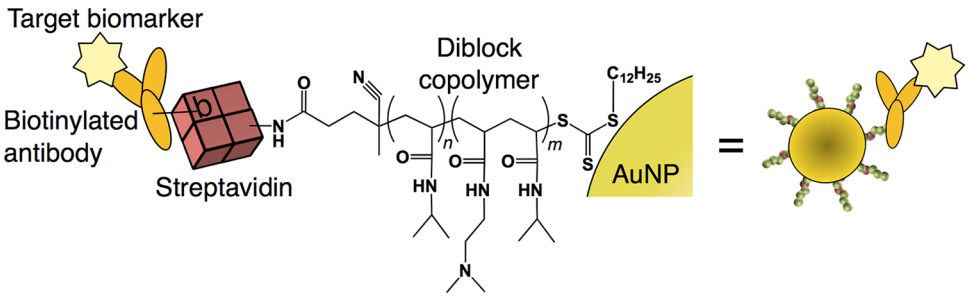

Figure 1. Targeted bioconjugate gold nanoparticle design. Gold nanoparticles were modified with a diblock copolymer produced *via* two-step RAFT polymerization. The polymer's semi-telechelic carboxyl group was conjugated to lysine groups on streptavidin, enabling linkage to a biotinylated affinity protein. This universal bioconjugate design allowed facile multiplexed detection by simply mixing different biotinylated antibodies with the sample before addition of the universal streptavidin-gold detection reagent.

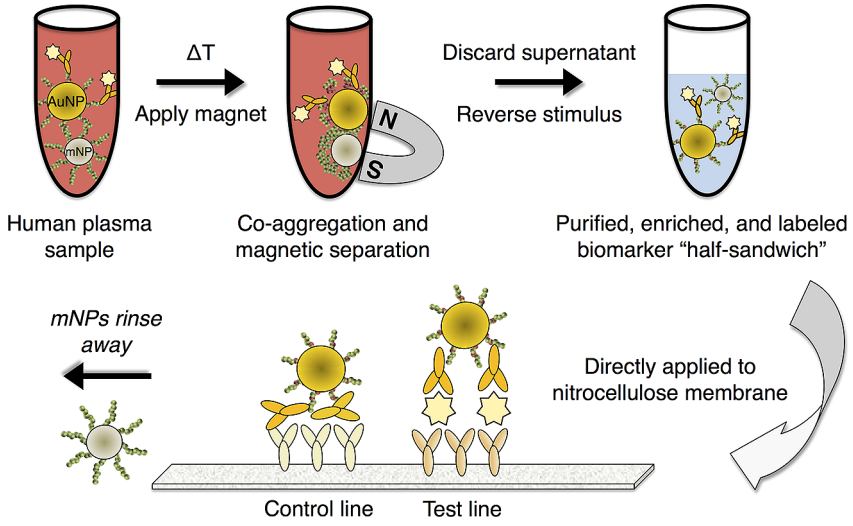

Figure 2. Depiction of the magnetic enrichment lateral flow immunoassay. A biotinylated antibody is added to a plasma sample containing the target biomarker(s). An equal volume of buffer containing streptavidin-pNIPAm-gold nanoparticles, pNIPAm magnetic nanoparticles, and free pNIPAm polymer is added. Upon heating, the mixed AuNP/mNP aggregates are separated by a magnet. After the supernatant is discarded, the captured aggregates are redissolved into a smaller volume of cool buffer, resulting in particle disaggregation and 50-fold enrichment. The enriched mixture is then applied directly to an immunochromatographic assay membrane with functionalized test and control line antibody regions.

354 nm and the IgG extinction coefficient of ε = 186 000 M^{-1} cm^{-1} at 280 nm, the measured absorbance ratio corresponded to 3−4 biotins per IgG. The degree of biotinylation of the anti-aldolase IgG used in the multiplexed assay was measured to be ~1−2 biotins per IgG using the same method. An overview of the active gold detection reagent complexed with the biotinylated antibodies is shown in Figure 1.

Magnetic Enrichment Lateral Flow Immunoassay. The magnetic enrichment lateral flow immunoassay proceeded in two modular steps, the first of which was the sample purification/enrichment, followed by the lateral flow immunochromatography readout, as depicted in Figure 2. Sample purification/enrichment was achieved by adding biotinylated antibodies to the spiked pooled plasma sample containing spiked PfHRP2 antigen molecules, followed by the SA-AuNP and pNIPAm-mNPs reagents. The thermal stimulus was then applied, causing polymer phase transitioning and nanoparticle coaggregation. Below the transition temperature, the non-aggregated mNPs were not separable in the magnetic field of a rare earth magnet.

Experiments were first performed to optimize the AuNP magnetic capture efficiency. We observed that higher separation efficiency was achieved by first applying the thermal stimulus in the absence of a magnetic field for 15 min. This allowed sufficient interaction time for the particles to form large aggregates of sufficient size to be magnetically separated. After this initial aggregation time, the turbid sample containing the coaggregated particle mixture was placed in close proximity to a magnet, resulting in magnetophoresis of the magnetic/gold particle aggregates. The effect of free polymer on AuNP capture efficiency is shown in Supplementary Figure 4. Typical AuNP capture efficiencies from 50% plasma using 1.5 mg/mL free polymer were >85% (Supplementary Figure 4).

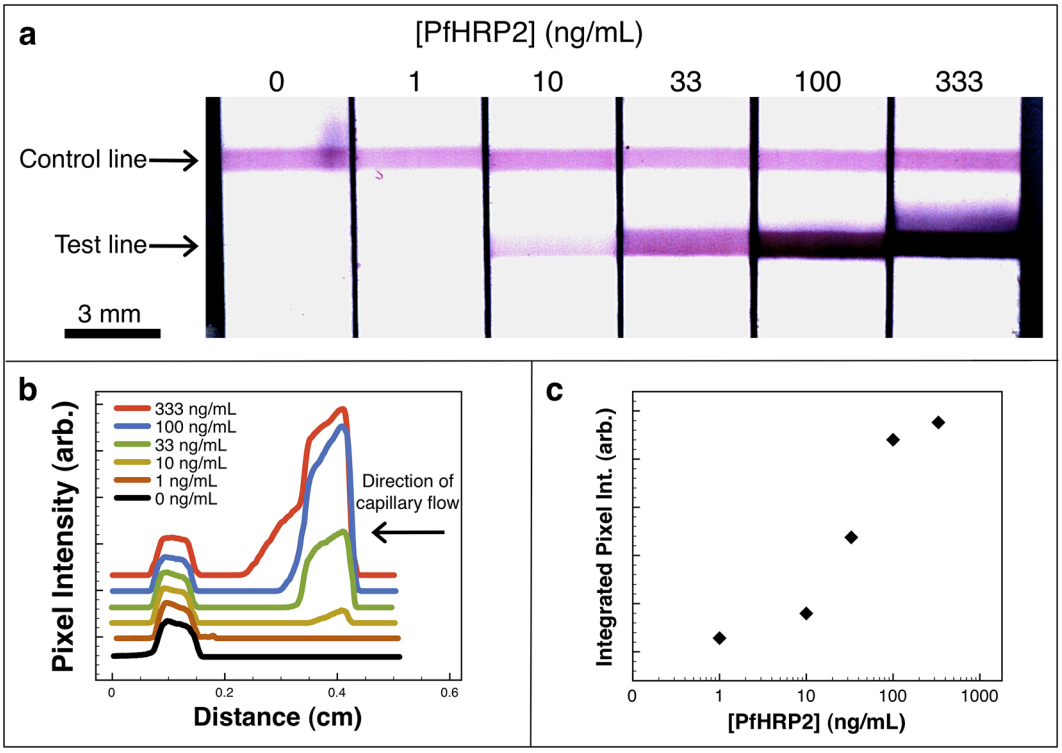

Figure 3. Recombinant PfHRP2 immunoassay. (a) Flow strip images, (b) green channel pixel intensity line scans offset along the *y*-axis for clarity, and (c) corresponding sigmoidal curve generated by a typical magnetic enrichment immunoassay performed on recombinant PfHRP2 biomarkers in spiked human plasma. The starting sample of 500 μL was magnetically enriched 50-fold prior to analyte visualization by immunochromatography.

After magnetic separation of the gold nanoparticles, the immunochromatography stage of the assay proceeded after removal of the supernatant and replacement with a smaller 10 μL volume of cold PBS buffer at pH 6.3. The slightly acidic pH of the resuspension buffer was chosen to protonate amine groups on the polymer and aid in the disaggregation of the AuNPs. Seven microliters of the enriched particle mixture was then applied directly to the cellulose fiber pad, and after 60 s, the rinse buffer was applied to chase the enriched particle mixture. Figure 3 shows typical flow strip images (a), line scans (b), and a standard sigmoidal curve generated using recombinant PfHRP2 biomarkers in spiked human plasma across a clinically relevant range. Line scans are offset along the *y*-axis for clarity.

The performance of the immunoassay with magnetic enrichment was evaluated for comparison purposes against the corresponding unmodified commercial lateral flow immunoassay. For the commercial assay, an equal volume (7 μL, 50% pooled plasma) containing the target PfHRP2 biomarker was applied to the dry gold conjugate pad through the sample application port of the flow strip cassette. After 60 s, the rinse buffer was applied to the buffer port, and the test was allowed to develop again for 6−7 min. Imaging and analysis were performed identically as for the magnetic enrichment immunoassay. Figure 4a shows scanned images obtained after performing a 50-fold enrichment assay (top row) or a conventional non-enriched assay (bottom row) with the commercial gold conjugate included in the flow strip cassette. In both cases, a 7 μL sample volume was applied to the flow strip. Visual inspection of the flow strips showed that the assay performed with 50-fold enrichment resulted in darker and thicker bands of gold colloid absorbance as compared with the assay performed without enrichment for a given biomarker concentration. Figure 4b is a plot of the green channel pixel intensity *versus* distance along the flow strip for the samples that were enriched 50-fold.

The signal at the test line for both the enriched and non-enriched sample flow strips was integrated and plotted (mean $\pm$ standard deviation, $n = 3$) as a function of the target biomarker concentration, as shown in Figure 4c. The signal response was 4.4 times steeper for the assay with 50-fold magnetic enrichment, determined by linear regression on the first three data points. The background noise of the assay at zero antigen was only marginally higher (0.54% increase) for the mixed nanoparticle processing and enrichment reagent system. A recombinant PfHRP2 concentration of 10 ng/mL was clearly visualized by the magnetic enrichment assay but was not detectable with the conventional flow strip. At 25 ng/mL, the commercial assay was only barely visible while the assay with 50-fold enrichment showed very strong

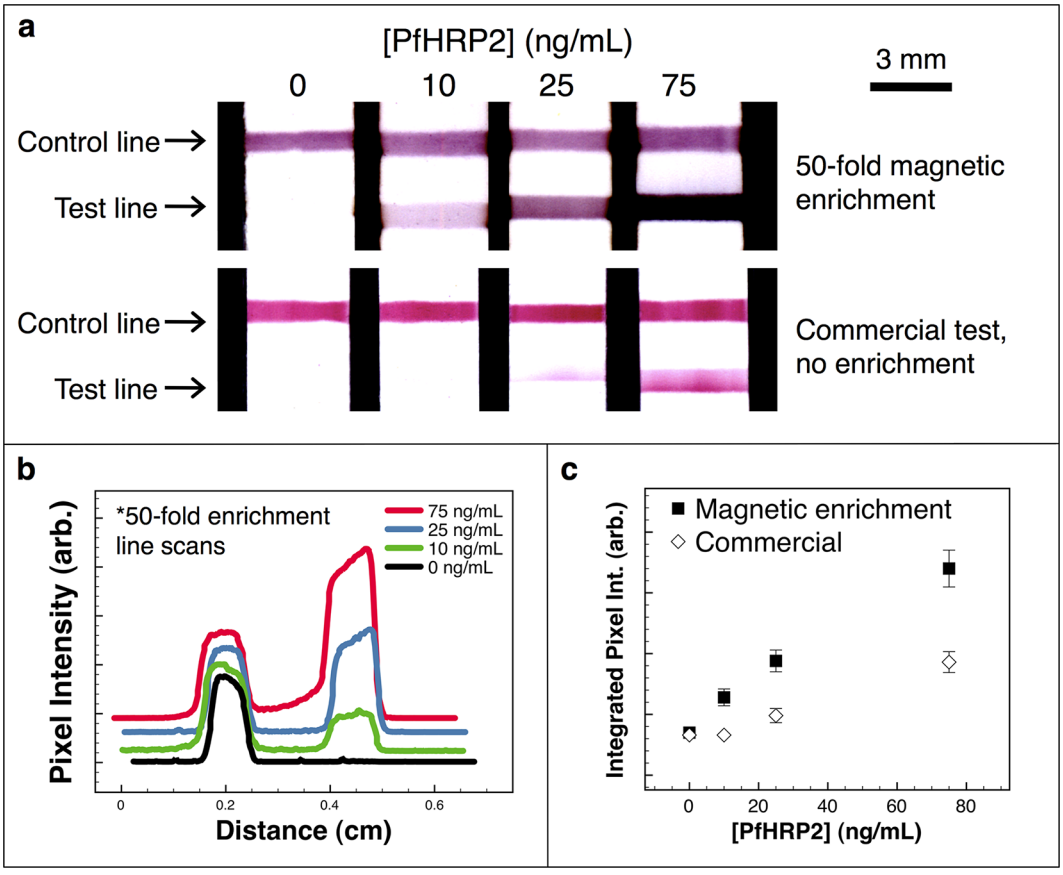

Figure 4. Comparison of magnetic enrichment and commercial assay. (a) Flow strip images from a 50-fold magnetic enrichment immunoassay (top row) and from the unmodified commercial assay performed with no enrichment (bottom row). (b) Green channel pixel intensity line scans for the magnetically enriched samples offset along the *y*-axis for clarity. (c) Integrated green channel pixel intensity at the test line plotted as mean ± standard deviation (n = 3) for the two assay systems.

signal. These results show how volumetric magnetic enrichment using the mixed magnetic/gold particle system can improve the sensitivity of lateral flow biosensors. Although our system lacked optimized surfactants, buffers, and highly selected matched antibody pairs, it performed better in signal level than the currently available commercial flow strips while maintaining the low zero background.

Effect of Increasing Sample Volume on Signal Generation. To demonstrate how volumetric enrichment can increase the test sensitivity, antigens derived from a human *Plasmodium falciparum* infection were spiked into pooled plasma and tested. Human plasma was collected by collaborators on site in Kisumu, Kenya, and shipped to Seattle, Washington, USA. The clinical plasma sample was tested by RT-qPCR and confirmed positive for *Plasmodium falciparum* infection. Microscopy analysis showed that the parasitemia level was approximately 451 000 parasites/μL. The sample was also tested for PfHRP2 protein by ELISA and found to be a strong positive. The reported parasitemia level is extremely high, which allowed us to spike small amounts of this specimen into larger pooled plasma samples to generate mock samples with moderate simulated parasitemia levels.

The clinical plasma sample was diluted into pooled human plasma (1:250) for all volumetric enrichment studies. The 1:250 dilution of the clinical PfHRP2 antigen was mixed sequentially with the biotinylated anti-PfHRP2 IgG antibody, the SA-AuNPs, the mNPs, and the homo-pNIPAm free polymer, resulting in a final sample composition of 50% pooled plasma (v/v). Samples were then split into 100 or 500 μL aliquots that were magnetically processed in parallel. After separation, the aggregates were resuspended into 10 μL of cold PBS buffer (pH 6.3), representing a 10-fold or 50-fold volumetric enrichment factor for the 100 and 500 μL sample aliquots, respectively. Seven microliters of the enriched particle mixtures was then applied to the flow strips and developed.

As shown in Figure 5a (top), the true positive result displaying two bands of AuNP absorbance (test and control lines) was only obtained for a processed sample volume of 500 μL. When a 100 μL volume was processed, no detectable signal at the test line was

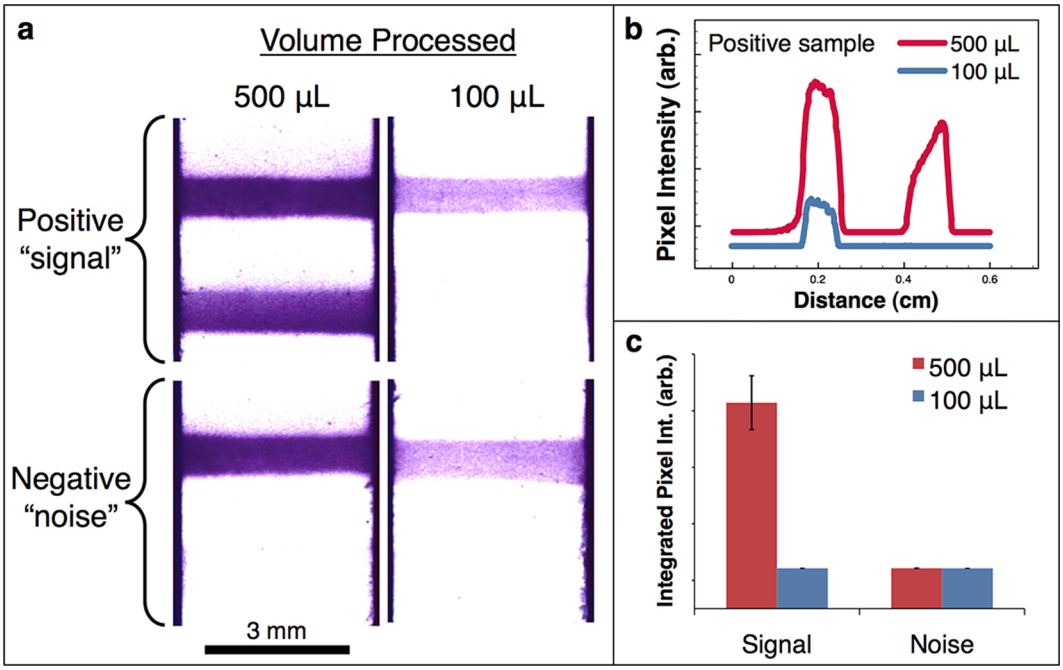

Figure 5. Effect of increasing sample volume on assay signal and noise. The PfHRP2 antigen was magnetically enriched from 100 or 500 μL volumes down to 10 μL, representing 10- or 50-fold volumetric enrichment, respectively. For the 100 μL processed volume, the magnetic enrichment immunoassay resulted in a false negative test result (a, top right), while for the 500 μL of processed sample (a, top left), a strong true positive signal at the test line was obtained. The assay noise remained low at each volume processed (a, bottom left and right). (b) Line scans from the positive sample, offset along the *y*-axis for clarity. (c) Integrated green channel pixel intensity at the test line (mean $\pm$ standard deviation, $n = 3$) for the positive ("signal") and negative ("noise") samples.

observed because the target biomarker in the 10-fold enriched sample was too dilute. The color at the control line was also darker for the 50-fold enriched sample due to an increase in the concentration of AuNPs. These observations demonstrate how volumetric enrichment by the nanoparticle mixtures boosts the signal for a highly relevant biomarker. Since the amount of signal generated is proportional to the total volume processed, stepwise incremental increases in signal for intermediate sample volumes from 200 to 500 μL were indeed observed and can be found in the Supplementary Figure 5.

We also assessed the effects of volumetric enrichment on the assay noise, as shown in Figure 5a (bottom). The pooled human plasma used as the diluent for the clinical antigen was tested without addition of the clinical PfHRP2 antigen molecules. The assay noise remained low at both 100 and 500 μL processed volumes of 50% plasma. Only a marginal increase in the assay noise was observed (<0.01%) for the 500 μL processed volume. That there is essentially no difference in the background noise regardless of the volume processed speaks to the high specificity of the antibodies and low nonspecific binding of the assay membranes. Shown in Figure 5b are line scans of the mean green channel pixel intensity plotted *versus* distance along the strip. The 500 μL processed volume shows the darkened pixel intensity at both test and control lines, while for the 100 μL processed volume, only the signal from the control line is seen. The line scans are offset on the *y*-axis for clarity. Figure 5c shows the integrated green channel pixel intensity (mean $\pm$ SD, $n = 3$) at the test line for the clinical PfHRP2 positive sample ("signal") and for the pooled plasma sample with no PfHRP2 ("noise"). The higher concentration of AuNP-reagent following magnetic enrichment did not increase background noise of the assay to any measurable degree.

Demonstration of Multiplexed Biomarker Enrichment and Detection. The advantages of multiplexed biomarker detection strategies have been demonstrated for a range of clinical diseases. Multiplexed detection is highly relevant in speciation of malarial infections and selection of the appropriate treatment course.[23] Taking advantage of the SA-AuNP labeling reagent, we demonstrated the ability of this modular system design to achieve multiplexed detection of malarial biomarkers from a single sample. Multiplexed detection of malarial antigens is clinically important and commonly used in diagnosing malaria infection in order to differentiate the multiple malaria species based on their specific PfHRP2 and pan-malarial aldolase biomarker expression profiles.[3] For multiplexed detection, recombinant PfHRP2 and pan-malarial aldolase antigens were spiked into pooled human plasma. Two different biotinylated antibodies, each specific for one of the two antigens, were then added and followed by addition of the SA-AuNPs (3 nM), mNPs

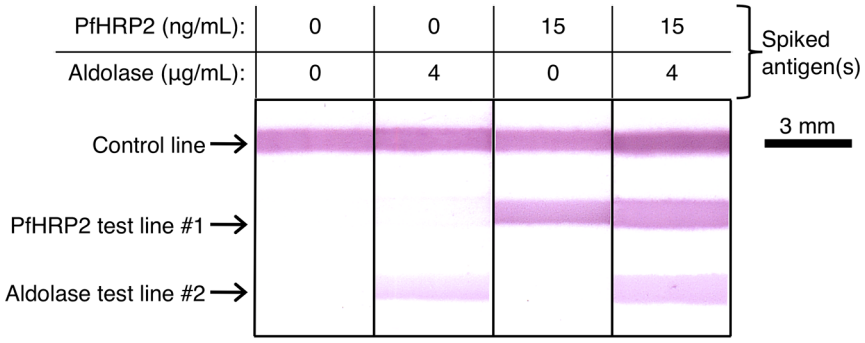

Figure 6. Multiplexed magneto-enrichment immunoassay. After binding of the biotinylated anti-PfHRP2 and anti-aldolase IgG antibodies to the mixed antigens in human plasma, the universal streptavidin-gold reagent was added, followed by magnetic enrichment and immunochromatographic readout. The top panel shows the respective concentrations of biomarkers in the original 500 μL sample.

(1 mg/mL), and homo-pNIPAm free polymer (2 mg/mL). The plasma was processed using the same heating and magneto-enrichment protocol described previously. The enriched particle mixture was flowed down the strip, sequentially through three capture lines. The line order (upstream to downsteam) was anti-aldolase, followed by anti-PfHRP2, and last the anti-mouse IgG control line. The lower sensitivity at the aldolase test line is likely due to a lower antibody affinity as the commercial strip and reagents showed the same trend. As shown in Figure 6, this assay allowed us to differentiate between plasma samples that had been spiked with neither, one, or both of the target biomarker species. These results demonstrate how the mixed AuNP/mNP system can be easily multiplexed without modifying either of the nanoparticle reagents.

CONCLUSIONS

The mixed stimuli-responsive AuNP/mNP system represents a new approach to achieving rapid isolation, labeling, and strong volumetric enrichment of AuNP-biomarker half-sandwich immunocomplexes. This is distinguished from conventional magnetic enrichment schemes, where the magnetic nanoparticle is conjugated to a targeting ligand and forms one side of the sandwich immunocomplex. Following purification and enrichment, AuNP-biomarker half-sandwiches could be applied directly to lateral flow test strips where they could bind to the complementary immobilized antibody at the immunospecific test line. Magneto-enrichment from larger sample volumes significantly boosted the test line signal without increasing assay noise on a spiked pooled plasma sample. The system could also be utilized for multiplexed biomarker detection as demonstrated with the pan-aldolase and PfHRP2 malarial antigens. This preprocessing/enrichment module based on the new mixed stimuli-responsive nanoparticle system provides a rapid method for biodetection applications where larger sample volumes are readily available and high-sensitivity immunochromatographic detection is required.

METHODS

Materials. *N*,*N*-Dimethylaminoethylacrylamide (DMAEAm; Monomer, Polymer, & Dajac Laboratories) was twice distilled prior to use. NIPAm (Sigma, 97%) was recrystallized from hexanes. 2,2-Azobis(2-methylpropionitrile) (AIBN; Aldrich, 98%) free radical initiator was recrystallized from methanol. The RAFT chain transfer agent 4-cyano-4-(dodecylsulfanylthiocarbonyl)sulfanyl pentanoic acid (DCT) was synthesized as described in the literature.[24] 2-(Dodecylsulfanylthiocarbonylsulfanyl)-2-methylpropionic acid (DMP) was a gift from Noveon. Dioxane (EMD, 99%), dimethylformamide (EMD, 99.8%), pentane (J.T. Baker, 99%), tetraglyme (Aldrich, 99%), methanol (MeOH; EMD, 99.9%), tetrahydrofuran (THF; Mallinckrodt, 99.8%), 1-ethyl-3-[3-dimethylaminopropyl]carbodiimide hydrochloride (EDC; Pierce, 98%), *N*-hydroxysulfosuccinimide (Sulfo-NHS; Pierce, 97%), $HAuCl_4$ (Aldrich, 99.99%), and NHS-chromogenic-biotin (Pierce, product #21325) were used as received. $Fe(CO)_5$ (Aldrich, 99.9%) was filtered through a 0.45 μm syringe filter. Phosphate buffered saline packets (1× PBS; 10 mM phosphate, 138 mM NaCl, 2.7 mM KCl, pH 7.4 at 25 °C) and 2-(*N*-morpholino)ethanesulfonic acid (100 mM MES, 100 mM NaCl) buffers were purchased from Sigma.

Polymer Synthesis. Reversible addition−fragmentation chain transfer (RAFT) polymerization was carried out using previously published procedures.[18,20] A homo-pNIPAm polymer with a target molecular weight of 15 kDa was first polymerized in a round-bottom flask. Then, 3.11 g (27.5 mmol) of NIPAm, 85 mg (0.212 mmol) of DCT, and 3.4 mg (20.8 μmol) of AIBN were mixed in 6 g of *p*-dioxane. The oxygen was removed by purging with N_2 for 30 min, followed by incubation at 60 °C for 18 h. The macro-chain-transfer agent (mCTA) product was obtained by precipitation into pentane, drying under vacuum, dialysis against DI water at 4 °C, and freeze-drying. Diblock chain extension was accomplished by dissolving in a round-bottom flask 2 g (117 μmol) of a 17.1 kDa homo-pNIPAm mCTA, 0.3 g (2.1 mmol) of DMAEAm, 0.2325 g (2.05 mmol) of NIPAm, and 1.9 mg (11.6 μmol) of AIBN in 8 mL of MeOH. This resulted in a [DMAEAm]/[NIPAm]/[mCTA]/[initiator] molar ratio of 18:18:1:0.1. The flask was purged with N_2 and heated to 60 °C for 18 h. After polymerization, the MeOH was removed by rotary evaporation, and the product dissolved in 5 mL of THF, followed by precipitation into pentane. The precipitate was dried under vacuum, dissolved in 15 mL of DI water, purified by PD-10 desalting column (GE Healthcare), and freeze-dried.

The lyophilized powder was dissolved at 10 mg/mL in DI water and further used for surface modification of AuNPs.

Polymer Analysis. Polymers were characterized using size exclusion chromatography performed on an Agilent 1200 series liquid chromatography system, equipped with TSKgel alpha 3000 and TSKgel alpha 4000 columns (TOSOH Biosciences). The mobile phase was LiBr (0.01 M) in HPLC grade DMF at a flow rate of 1 mL/min. Multiangle light scattering data were obtained on a miniDAWN TREOS (Wyatt Technologies Corp.) with a 658 nm laser source and three detectors at 45.8, 90.0, and 134.2°. The instrument calibration constant was 4.7460×10^{-5} V^{-1} cm^{-1}. The refractive index was measured using an Optilab Rex detector (Wyatt Technologies Corp.). The d*n*/d*c* value for the homo-pNIPAm mCTA was determined under an assumption of 100% mass recovery, while the d*n*/d*c* value for the diblock copolymer was determined by injecting polymer samples at known concentrations into the RI detector postcolumn. The diblock d*n*/d*c* value was then calculated using linear regression with the Astra 5.3.4.14 data analysis software package (Wyatt Technologies Corp.). ^{1}H NMR (300 MHz) spectroscopy in $CDCl_3$ was performed on a Bruker AV300. ^{1}H NMR performed in $CDCl_3$ confirmed the polymer chemical composition with the DMAEAm peak observed at δ(ppm) = 2.26 (s, R-N(CH_3)$_2$) and NIPAm peaks at δ(ppm) = 1.15 (s, R-CO-NH−CH-(CH_3)$_2$) and at 4.00 (s, R-CO-NH-C<u>H</u>-(CH_3)$_2$) with an integrated peak ratio of ∼6:1.

Magnetic Nanoparticle Synthesis. Magnetic nanoparticles (mNPs) with a 5 kDa homo-pNIPAm corona were synthesized as previously described.[18−20] Briefly, the 5 kDa homo-pNIPAm was dissolved in tetraglyme (3.6 mM) at 100 °C. Next, 4 μL of $Fe(CO)_5$ per mL of tetraglyme was added to the polymer/tetraglyme mixture at 100 °C. The temperature was then raised to 180 °C for 5 h. The reaction was cooled, and the mNPs were obtained by precipitation into pentane, drying under vacuum, dialysis against DI water at 4 °C, and freeze-drying. The dried product was then dissolved in DI water at 50 mg/mL and stored at 4 °C for up to 3 months prior to use. Particle diameter was determined to be ∼10 nm using a combination of dynamic light scattering (DLS) and transmission electron microscopy (TEM). DLS was performed on a Brookhaven BI90Plus with a 535 channel correlator and 656 nm laser source at 90° scattering angle. TEM samples were prepared by dissolving particles in DI water at 3 mg/mL. Particle solutions were aerosolized onto carbon-stabilized Formvar-coated copper grids (Ted Pella) using a spray bottle. Imaging was performed on a Technai G2 F20 200 kV scanning transmission electron microscope.

Gold Nanoparticle Synthesis. Citrate-stabilized colloidal gold was prepared according to the literature.[25] All glassware was cleaned with aqua regia, thoroughly rinsed with DI water, and dried before use. Next, 150 mL of 0.1 mg/mL $HAuCl_4$ was brought to a boil in a round-bottom flask. Then, 1.76 mL of 10 mg/mL sodium citrate in DI water was rapidly added. The reaction was boiled under reflux for 30 min and cooled to room temperature. The pH was raised to 8.2 by addition of 0.1 M NaOH. Next, 1.2 mL of a 10 mg/mL solution of 21.5 kDa diblock copolymer in DI water was added. The flask was purged with N_2 for 45 min and stirred at 22 °C for 24 h in darkness. Next, 1 g of NaCl was added, followed by an additional 24 h of stirring at 22 °C. The particles were then concentrated under 35−40 psi of N_2 using a membrane ultrafiltration system with a cellulose membrane from Millipore (regenerated cellulose, 44.5 mm diameter, NMWL 100 000, product #14422AM). The polymer-modified AuNPs were washed off the membrane with 2 mL of 0.1 M MES buffered saline at pH 5.0. The AuNPs in MES buffer were then used for NHS-ester activation and conjugation to streptavidin within 24 h. The nanoparticles had pseudospherical morphology with a diameter of ∼25 nm determined by combined DLS and TEM (Supplementary Figures 6 and 7). Gold nanoparticle absorption was measured on a Hewlett-Packard 8453 diode array extinction spectrophotometer with a temperature-controlled quartz cuvette sample holder. Phase-separation temperature of the magnetic nanoparticles can be found in the Supporting Information (Supplementary Figure 8). Red-shifting of the localized surface plasmon resonance (LSPR) upon phase separation of the AuNPs is shown in Supplementary Figure 9. Thermogravimetric analysis was performed on a Perkin-Elmer TGA7 instrument (Supplementary Figure 10). Thermogravimetric analysis of the diblock modified AuNPs showed they were 93% inorganic content by weight. The mNPs were found to be 7.4% inorganic content by weight.

Conjugation of Gold Nanoparticles to Streptavidin. Two milliliters of the diblock copolymer-modified AuNP solution (∼70 nM in MES buffered saline at pH 5.0) was added to 13.1 mg of sulfo-NHS and 14.8 mg of EDC in dry form. The NHS-ester activation proceeded for 40 min at room temperature with orbital shaking. Buffer exchange was performed with a centrifugal size exclusion column (Zeba desalting spin column, Pierce) to transfer the AuNPs to 1× PBS 7.3 buffer. The NHS-activated AuNPs were then added to lyophilized streptavidin (U.S Biological, Swampscott, MA) and allowed to react overnight at room temperature with orbital shaking. After conjugation to streptavidin, the reaction volume was increased to 50 mL with 1× PBS 7.3 buffer. The 50 mL volume was concentrated using membrane ultrafiltration as described above. This dilution/concentration process was repeated two more times, while the absorbance of the flow through eluent was monitored at 280 nm to confirm the removal of nonconjugated streptavidin. The final product (SA-AuNPs) was rinsed off the membrane with PBS buffer, pH 7.3. The SA-AuNPs were stored (∼80 nM) in PBS at 4 °C under N_2 for up to 3 months and used for further immunoassay studies.

Biotinylation of Anti-PfHRP2 IgG and Anti-Aldolase IgG Antibodies. Monoclonal mouse anti-PfHRP2 IgG (product #MPFG-55A) and monoclonal mouse anti-aldolase IgG (product #RPVA-55A) were purchased from Immunology Consultants Laboratory (Newberg, OR). Modification of the IgG antibodies was performed using an NHS-activated biotin containing a chromophore linker. The NHS-chromogenic-biotin (Pierce, Rockford, IL) dissolved at 10 mg/mL in anhydrous dimethylformamide was added in 7.5 molar excess to the IgG protein at 1 mg/mL in PBS buffer, pH 7.3, at room temperature. After 3 h, the unreacted NHS-chromogenic-biotin was removed using a centrifugal size exclusion column (Zeba desalting column, Pierce). The degree of biotinylation was estimated by measuring the ratio of the biotin-chromophore extinction (ε = 29 000 M^{-1} cm^{-1} at 354 nm) to the IgG extinction (ε = 186 000 M^{-1} cm^{-1} at 280 nm).

Lateral Flow Device Modification. Commercial immunochromatography devices with a control line of anti-mouse antibody and two test lines of anti-aldolase and anti-PfHRP2 antibodies were purchased from Sanitoets Sallamander Concepts CC (Lynnwood Pretoria, South Africa). The commercial flow strips were removed from the plastic cassette, and the dried gold conjugate pad was carefully removed and discarded. The assay membrane was then remounted onto a strip of adhesive-coated mylar (4 mm wide × 38 mm long). A porous rectangular sheet of cellulose fiber (4 × 5 mm, grade #8301, Ahlstrom, Mount Holly Springs, PA) was placed on the assay membrane upstream of the capture lines to serve as a filter and liquid reservoir for the nanoparticle mixtures, while the sample liquid was imbibed by the nitrocellulose membrane. A cellulose absorbent pad (4 × 10 mm) was placed just upstream of the assay membrane to serve as a rinse buffer reservoir.

Magnetic Enrichment Lateral Flow Immunoassay Protocol. Pooled human plasma in disodium EDTA (Valley Biomedical Inc., product #HP1051) was centrifuged at 1000*g* for 30 min and filtered through GDX graded syringe filters (Whatman) prior to use. A recombinant pan-malarial aldolase antigen (product #AGPV-55) and a recombinant PfHRP2 antigen (product #AGPF-55) were purchased from Immunology Consultants Laboratory (Newberg, OR). A clinically derived plasma sample containing the PfHRP2 antigen was obtained onsite in Kisumu, Kenya, through a collaboration between the PATH (Seattle, WA), the Walter Reed Army Institute of Research (WRAIR), and the Kenyan Medical Research Institute (KEMRI) through a study reviewed and approved by the following institutional review boards: Kenya Ethical Review Committee ERC #1117, WRAIR HURC #1315, and PATH Research Ethics Committee HS #358.[26] Blood smear histology was used to estimate the parasitemia level, which was found to be 451 000 parasites/μL for the sample used in this report. The sample was confirmed positive for 16s rRNA of *Plasmodium falciparum* (sequences proprietary) using real-time

quantitative PCR. The clinical sample was also tested and found positive for PfHRP2 protein by ELISA. For the clinical antigen, 1 μL of PfHRP2-positive clinical plasma was diluted into 250 μL of pooled human plasma, resulting in a simulated parasitemia level of 1804 parasites/μL. For assays using recombinant antigen(s), the antigens were spiked into 250 μL of pooled plasma. One nanomolar of the biotinylated anti-PfHRP2 IgG antibodies was then added to the pooled human plasma, followed sequentially by PBS at pH 8.3, SA-AuNPs (2 nM), homo-pNIPAm mNPs (1 mg/mL), and 8 kDa homo-pNIPAm free polymer (1.5 mg/mL). The total volume of the sample after addition of all reagents was 500 μL (*i.e.*, 50% plasma (v/v)). For multiplexed detection of PfHRP2 and aldolase, 1 nM of anti-aldolase IgG was also included in the reaction mixture.

Coaggregation of the thermally responsive magnetic and gold nanoparticle mixtures was achieved by heating for 15 min up to to 40 °C with gentle orbital shaking in an aluminum tube holder equilibrated inside an incubator. The sample was then incubated at 40 °C for an additional 15 min in close contact with a rare earth magnet (NdFeB, 1.27 × 0.63 cm, 12.1 kGauss). Next, the supernatant was carefully removed and discarded with a pipet, and the AuNP/mNP aggregates captured along the wall of the Eppendorf tube were redissolved in 10 μL of 1× PBS buffer (pH 6.3, 4 °C), resulting in 50-fold volumetric enrichment. Seven microliters of the enriched particle mixture was then applied onto the cellulose fiber pad sitting atop the lateral flow assay membrane. The liquid was allowed to wick into the strip for 60 s, after which, 60 μL of the rinse buffer included in the commercial kit was applied to chase the AuNP/mNP mixture. The test was allowed to develop for 6−7 min in total, followed by removal of the absorbent pads, air drying, and imaging.

Image Acquisition and Analysis. Lateral flow membranes were mounted onto glass slides and imaged using a flatbed scanner (ScanMaker i900, MicroTek International, Inc.) at 900 dpi in 48-bit RGB mode. Images of the flow strips were analyzed using the NIH Image J software package. The integrated green channel pixel intensity at the anti-PfHRP2 test line of the lateral flow membranes was measured as a function of recombinant biomarker concentration to generate a standard curve. All samples were run in triplicate and plotted as mean ± standard deviation.

Conflict of Interest: The authors declare no competing financial interest.

Acknowledgment. M.A.N. gratefully acknowledges funding from the National Science Foundation Graduate Research Fellowship Program (NSF-GRFP), and from the Alexander von Humboldt Foundation Postdoctoral Research Fellowship Program, Germany. The Kenyan Medical Research Institute, the Walter Reed Army Institute of Research, and the Program for Appropriate Technology in Health (PATH, Seattle, WA) are gratefully acknowledged for collection and analysis of clinical samples. This work was supported by the National Institutes of Health (Grant EB000252), and through funding from The Bill & Melinda Gates Foundation's Grand Challenges in Global Health Initiative under Grant Number 37884, "A Point-of-Care Diagnostic System for the Developing World", awarded to the UW-led consortium: P.Y., PI (UW) and collaborators at Micronics Inc., Epoch BioSciences, PATH, and the Stayton Group (UW).

Supporting Information Available: The ^{1}H NMR spectrum of the polymer (Supplementary Figure 1), thermal aggregation profile of the polymer (Supplementary Figure 2), streptavidin absorbance depletion (Supplementary Figure 3), effect of free polymer on AuNP capture efficiency (Supplementary Figure 4), stepwise increase in signal for the clinical sample (Supplementary Figure 5), TEM micrographs of nanoparticles (Supplementary Figures 6 and 7), phase transition of the magnetic nanoparticles (Supplementary Figure 8), red-shifting of the plasmon resonance of the AuNPs upon phase separation (Supplementary Figure 9), thermogravimetric analysis of nanoparticle samples (Supplementary Figure 10), and extended materials and methods are available as Supporting Information. This material is available free of charge *via* the Internet at http://pubs.acs.org.

REFERENCES AND NOTES

1. Giljohann, D. A.; Mirkin, C. A. Drivers of Biodiagnostic Development. *Nature* **2009**, *462*, 461–464.
2. Posthuma-Trumpie, G. A.; Korf, J.; van Amerongen, A. Lateral Flow (Immuno) Assay: Its Strengths, Weaknesses, Opportunities and Threats. A Literature Survey. *Anal. Bioanal. Chem.* **2009**, *393*, 569–582.
3. Moody, A. Rapid Diagnostic Tests for Malaria Parasites. *Clin. Microbiol. Rev.* **2002**, *15*, 66–78.
4. Beadle, C.; Long, G. W.; Weiss, W. R.; McElroy, P. D.; Maret, S. M.; Oloo, A. J.; Hoffman, S. L. Diagnosis of Malaria by Detection of *Plasmodium falciparum* Hrp-2 Antigen with a Rapid Dipstick Antigen-Capture Assay. *Lancet* **1994**, *343*, 564–568.
5. Bell, D.; Peeling, R. W. Evaluation of Rapid Diagnostic Tests: Malaria. *Nat. Rev. Microbiol.* **2006**, S34–S40.
6. Laderman, E. I.; Whitworth, E.; Dumaual, E.; Jones, M.; Hudak, A.; Hogrefe, W.; Carney, J.; Groen, J. Rapid, Sensitive, and Specific Lateral-Flow Immunochromatographic Point-of-Care Device for Detection of Herpes Simplex Virus Type 2-Specific Immunoglobulin G Antibodies in Serum and Whole Blood. *Clin. Vaccine Immunol.* **2008**, *15*, 159–163.
7. Yager, P.; Edwards, T.; Fu, E.; Helton, K.; Nelson, K.; Tam, M. R.; Weigl, B. H. Microfluidic Diagnostic Technologies for Global Public Health. *Nature* **2006**, *442*, 412–418.
8. Hauck, T. S.; Giri, S.; Gao, Y. L.; Chan, W. C. W. Nanotechnology Diagnostics for Infectious Diseases Prevalent in Developing Countries. *Adv. Drug Delivery Rev.* **2009**, *62*, 438–448.
9. Gordon, J.; Michel, G. Analytical Sensitivity Limits for Lateral Flow Immunoassays. *Clin. Chem.* **2008**, *54*, 1250–1251.
10. Malmstadt, N.; Hoffman, A. S.; Stayton, P. S. "Smart" Mobile Affinity Matrix for Microfluidic Immunoassays. *Lab Chip* **2004**, *4*, 412–415.
11. Auditore-Hargreaves, K.; Houghton, R. L.; Monji, N.; Priest, J. H.; Hoffman, A. S.; Nowinski, R. C. Phase-Separation Immunoassays. *Clin. Chem.* **1987**, *33*, 1509–1516.
12. Fong, R. B.; Ding, Z. L.; Long, C. J.; Hoffman, A. S.; Stayton, P. S. Thermoprecipitation of Streptavidin *via* Oligonucleotide-Mediated Self-Assembly with Poly(*N*-isopropylacrylamide). *Bioconjugate Chem.* **1999**, *10*, 720–725.
13. Mori, T.; Umeno, D.; Maeda, M. Sequence-Specific Affinity Precipitation of Oligonucleotide Using Poly(*N*-isopropylacrylamide)-Oligonucleotide Conjugate. *Biotechnol. Bioeng.* **2001**, *72*, 261–268.
14. Ossendorp, F. A.; Bruning, P. F.; Vandenbrink, J. A. M.; Deboer, M. Efficient Selection of High-Affinity B-Cell Hybridomas Using Antigen-Coated Magnetic Beads. *J. Immunol. Methods* **1989**, *120*, 191–200.
15. Treleaven, J. G.; Gibson, F. M.; Ugelstad, J.; Rembaum, A.; Philip, T.; Caine, G. D.; Kemshead, J. T. Removal of Neuroblastoma Cells from Bone-Marrow with Monoclonal-Antibodies Conjugated to Magnetic Microspheres. *Lancet* **1984**, *1*, 70–73.
16. Gijs, M. A. M.; Lacharme, F.; Lehmann, U. Microfluidic Applications of Magnetic Particles for Biological Analysis and Catalysis. *Chem. Rev.* **2010**, *110*, 1518–1563.
17. Chen, G. D.; Alberts, C. J.; Rodriguez, W.; Toner, M. Concentration and Purification of Human Immunodeficiency Virus Type 1 Virions by Microfluidic Separation of Superparamagnetic Nanoparticles. *Anal. Chem.* **2010**, *82*, 723–728.
18. Lai, J. J.; Hoffman, J. M.; Ebara, M.; Hoffman, A. S.; Estournes, C.; Wattiaux, A.; Stayton, P. S. Dual Magnetic-/Temperature-Responsive Nanoparticles for Microfluidic Separations and Assays. *Langmuir* **2007**, *23*, 7385–7391.
19. Lai, J. J.; Nelson, K. E.; Nash, M. A.; Hoffman, A. S.; Yager, P.; Stayton, P. S. Dynamic Bioprocessing and Microfluidic Transport Control with Smart Magnetic Nanoparticles in Laminar-Flow Devices. *Lab Chip* **2009**, *9*, 1997–2002.
20. Nash, M. A.; Lai, J. J.; Hoffman, A. S.; Yager, P.; Stayton, P. S. "Smart" Diblock Copolymers as Templates for

Magnetic-Core Gold-Shell Nanoparticle Synthesis. *Nano Lett.* **2010**, *10*, 85–91.
21. Nash, M. A.; Yager, P.; Hoffman, A. S.; Stayton, P. S. Mixed Stimuli-Responsive Magnetic and Gold Nanoparticle System for Rapid Purification, Enrichment, and Detection of Biomarkers. *Bioconjugate Chem.* **2010**, *21*, 2197–2204.
22. Fustin, C. A.; Duwez, A. S. Dithioesters and Trithiocarbonates Monolayers on Gold. *J. Electron Spectrosc. Relat. Phenom.* **2009**, *172*, 104–106.
23. Fu, Q.; Schoenhoff, F. S.; Savage, W. J.; Zhang, P. B.; Van Eyk, J. E. Multiplex Assays for Biomarker Research and Clinical Application: Translational Science Coming of Age. *Proteomics: Clin. Appl.* **2010**, *4*, 271–284.
24. Moad, G.; Chong, Y. K.; Postma, A.; Rizzardo, E.; Thang, S. H. Advances in Raft Polymerization: The Synthesis of Polymers with Defined End-Groups. *Polymer* **2005**, *46*, 8458–8468.
25. Frens, G. Controlled Nucleation for Regulation of Particle-Size in Monodisperse Gold Suspensions. *Nat. Phys. Sci.* **1973**, *241*, 20–22.
26. Waitumbi, J. N.; Gerlach, J.; Afonina, I.; Anyona, S. B.; Koros, J. N.; Siangla, J.; Ankoudinova, I.; Singhal, M.; Watts, K.; Polhemus, M. E.; *et al.* Malaria Prevalence Defined by Microscopy, Antigen Detection, DNA Amplification and Total Nucleic Acid Amplification in a Malaria-Endemic Region during the Peak Malaria Transmission Season. *Trop. Med. Int. Health* **2011**, *16*, 786–793.